Mater. Res. Soc. Symp. Proc. Vol. 1397 © 2012 Materials Research Society
DOI: 10.1557/opl.2012.259

Kinetics of palladium particles on $LiNbO_3$: an origin of the polarization-dependent catalysis

Seungchul Kim, Michael Rutenberg Schoenberg and Andrew M. Rappe
The Makineni Theoretical Laboratories, Department of Chemistry, University of Pennsylvania, Philadelphia, PA 19104-6323, U.S.A.

ABSTRACT

Using *ab-initio* calculations and kinetic Monte Carlo simulations, we demonstrate that the deposition geometries of palladium are strongly dependent on the polarization direction of the $LiNbO_3$ substrate. Different stoichiometries and atomic structures of the positively and the negatively polarized substrates cause substantially different bonding configurations of palladium and energy barriers for the movement of Pd clusters. Our simulations predict that palladium atoms form bulky clusters on the positive surface, while they are deposited in a dispersed or planar manner on the negative surface at moderate temperature. We suggest that Inoue and coworkers' observation [*J. Phys. Chem.* **88**, 1148 (1984)] that the catalytic activity of palladium depends on polarization direction of $LiNbO_3$ substrate is, at least in part, due to differences in the geometric structures of palladium and the $LiNbO_3$ surface.

INTRODUCTION

A transition metal that is supported on a ferroelectric oxide is a special subcategory of metal-supported oxides, which are widely used as heterogeneous catalysts. However, it has been expected that a ferroelectric support has one degree of freedom that may alter catalytic activity: switchable polarization. Inoue and coworkers demonstrated this idea in 1984 [1]; they showed that the activation barriers of CO oxidation differ by 30 kJ/mol when the reactions are catalyzed by Pd supported on the positively and the negatively poled lithium niobate ($LiNbO_3$) substrates. The traditional explanation of polarization-dependent catalysis is that the opposite signs of surface charges on oppositely polarized surfaces alter the electronic structure of the supported metal differently; in turn, catalytic activity will be changed.

However, surface charges of any polarized materials must be passivated to prevent the divergence of the electrostatic potential energy [2]. Thus, there might not be enough surface charge to alter the electronic structure of the catalytic metal. Then, what could alter the activity of this kind of catalyst? Since the catalytic activity of a transition metal can be affected both electronically and geometrically [3], we speculate that this activity difference is more geometric in origin rather than electronic. In fact, it has been experimentally demonstrated that particle sizes of Pd are different when deposited on the positive and negative surfaces of $LiNbO_3$ (0001) [4, 5]. Furthermore, polarization-dependent CO temperature programmed desorption (TPD) is found in the cases that show large differences in particle size [4]. These experiments seem to support our speculation.

We investigate whether and how the polarization direction of the $LiNbO_3$ (0001) substrate affects the geometric structure of deposited Pd. First, we tested the adsorption and diffusion characters of small Pd clusters using density functional theory (DFT) calculations.

Then, we used these results to parameterize kinetic Monte Carlo (KMC) simulations of the deposition process, to investigate cluster growth in various conditions.

COMPUTATIONAL DETAILS

Ferroelectric $LiNbO_3$ consists of, from the positive to the negative direction, stacked Li-O_3-Nb trilayers [6]. In all DFT calculations, we modeled $LiNbO_3$ (0001) surfaces as five-trilayer thick slabs with $\sqrt{3} \times \sqrt{3}$ surface supercell. Surface charge was passivated by one extra Li ion per 1×1 surface unit cell for the c^+ surface, and by one Li and one O ions for the c^- surface, as Levechenko and Rappe have predicted [7]. Thus the compositions are Li_2-(O_3-Nb-Li)$_n$ and LiO-(Nb-O_3-Li)$_n$ for c^+ and c^- surfaces, respectively. Figure 1a shows the side view of the slabs used in the calculations. We applied the GGA-PBE exchange-correlation energy functional [8], a plane-wave basis set with 50 Ry cutoff, and optimized norm-conserving pseudopotentials [9, 10]. Transition paths and barriers were calculated using the climbing image nudged elastic band (CI-NEB) method [11]. We used Quantum ESPRESSO [12] for all DFT calculations. Up to five-atom clusters were tested to find their adsorption geometries, adsorption energies, bonding characters, dissociation barriers, and diffusion barriers. We also tested single atomic motions in the large cluster using single-atomic-layer-thick Pd ribbons on the $LiNbO_3$ surfaces, and an isolated large cluster.

Our KMC simulations for Pd deposition were carried out in the three-dimensional lattice of fixed Pd sites, which consists of stacked two-dimensional triangular lattices. Each lattice plane contains three triangular sublattices, so that the lattice can describe Pd atoms that occupy either face-centered cubic (FCC) or hexagonal closed packed (HCP) sites; even though Pd bulk is FCC, HCP sites are also necessary to describe motions of atoms and clusters. We allowed diffusion processes of up to four-atom clusters: hopping, sliding, and rolling. We included single-atomic internal motions of clusters to describe cluster shape change such as agglomeration. To model deposition, Pd atoms were added at random locations with fixed time interval during the simulations. The events were chosen probabilistically; the characteristic time (τ_i) and probability ($P_i(t)$) that event i will be happen before time t elapses is given by equation (1) and (2) [13].

$$P_i(t) = 1 - e^{-t/\tau_i} \qquad (1)$$

$$\frac{1}{\tau_i} = \nu e^{-E_i/k_B T} \qquad (2)$$

Here, E_i is the activation barrier of the event i; v is the attempt frequency of the event; k_B is the Boltzmann constant; and T is the temperature. We used constant attempt frequency (v=10^{12} sec^{-1}) for all events.

DISCUSSION

Adsorption geometries and energies of small clusters

Our DFT calculations predicted that palladium atoms mostly bond with the surface oxygen atoms on both the positive (c^+) and the negative (c^-) surfaces of $LiNbO_3$ (0001). Wave functions and density of states (DOS) analysis revealed that the bonds between Pd and the substrates are the same type; Pd covalently bonds to the surface oxygen rather than making ionic

bonds. Additionally, the energy of the Pd 4*d* orbitals relative to the Fermi energy, an important predictor of catalytic activity [14], is very similar for Pd on the c^+ and c^- surfaces.

However, because of the difference in atomic structure between two surfaces (Figure 1), Pd atoms are differently adsorbed, both geometrically and energetically. On the c^+ surface, Pd atom can bond with only one O atom (Figure 1c), while it can bond with two O atoms on the c^- surface due to the flexible O-Nb bonds (Figure 1e). The outermost O atom on c^- forms a chemical bond with only one Nb atom (Figure 1a), thus the O-Nb bond is easy to tilt. The different number of Pd-O bonds causes substantially different Pd adsorption geometries and energies. For example, adsorption energies of the Pd monomer on c^+ is 0.95 eV, while that on c^- is 2.02 eV, a factor of two difference that is reasonable from counting the Pd-O bonds. As they increase in size, Pd clusters become agglomerated on c^+, to maximize the number of inter-palladium bonds. On the other hand, at least up to five-atom clusters, planar and three-dimensional clusters on c^- have very similar energies, due to more Pd-O bonds. Interestingly, for c^-, we found that both Pd-O and Pd-Pd bonds are very similar, and the averaged bond strength for Pd_1 – Pd_5 is 1.03 ± 0.05 eV. This finding provides us with a simple model for Pd adsorption and motion on c^-, which will be discussed later.

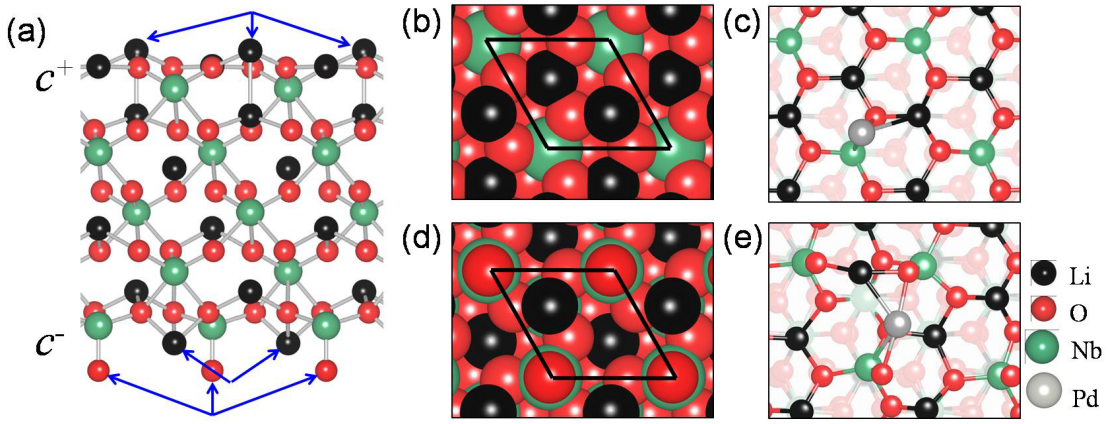

Figure 1 Atomic structure of $LiNbO_3$ (0001) surface: (a) is a side view of the five-trilayer slab used in the DFT calculations, (b) top view of c^+ surface, (c) Pd monomer adsorption geometry on c^+, (d) top view of c^-, and (e) Pd monomer adsorption geometry on c^-. Blue arrows in (a) indicate the extra ions that passivate surface charge, and black lines in (b) and (c) indicate 1×1 surface unit cell. Reproduced with permission from ref [15].

Diffusion processes of small clusters and deposition structures

The potential energy surface (PES) of the Pd monomer on the c^+ surface is shallow; the maximum energy position is 0.7 eV from the minimum, and the highest saddle point (i.e. transition state) is 0.39 eV, which is the diffusion barrier of the monomer. Diffusion barriers of Pd_2 – Pd_4 are comparable with that of the monomer because there are many diffusion processes that are practically single atomic motions; the walking motion of Pd_2 and rolling of tetrahedral Pd_4 are representative examples of those. In the walking process, one atom of a dimer jumps to the next stable position while the other does not move. Tetrahedral Pd_4 consists of three atoms at the bottom and one atom on the hollow site of the bottom three. During the rolling process, only one atom breaks its bonds to the substrate, while the other two bottom atoms stay at their original positions. Mismatch between PES periodicity and preferred Pd-Pd bond length lowers some barriers, and causes deviation of the diffusion barriers from the monomer's barrier. We also

found that the agglomeration barrier, which is the energy required to be convert from a two-dimensional structure to a three-dimensional structure, is negligible for c^+.

For the c^- surface, the PES of the monomer cannot be applied to cluster adsorption due to the relatively flexible O-Nb bonds. Instead, counting the number of Pd-O bonds formed or broken is better to understand diffusion processes. Pd-O and Pd-Pd bonding energies are each about 1 eV, and any diffusion requires at least one Pd-O or Pd-Pd bond to break. These facts help us understand the size of the energy barriers for cluster diffusion, dissociation, and agglomeration. Diffusion barriers are about 0.8 eV or larger (Table 1); the Pd_2 dissociation barrier is 0.77 eV; agglomeration barriers are 0.54 – 0.93 eV. The barriers change from about 1 eV because a new bond starts to form before the bond that causes the barrier is completely broken, or because other bonds are concurrently changed. About 1 eV of bonding strength also justifies our KMC model that the tetramer is the largest mobile species; clusters larger than tetramer need multiple bonds to break in order to diffuse, and this bond breaking requires a very large activation barrier.

Table 1 Diffusion barriers, in eV, of Pd clusters on the c^+ and c^- surfaces. The minimum and maximum values are listed.

	Pd_1	Pd_2	Pd_3	Pd_4
c^+	0.09 – 0.39	0.02 – 0.41	0.11 – 0.46	0.06 – 0.40
c^-	0.82 – 0.87	1.06	1.30 – 1.31	0.70 – 0.85

Kinetic explanation of Pd deposition

Differences in DFT predicted diffusion barriers (E_a), ≤ 0.4 eV for c^+ and ≥ 0.8 eV for c^-, are large enough to give rise to a substantial difference in the kinetic time scale between oppositely poled surfaces. Assuming attempt frequency ν=10^{12} sec^{-1}, Arrhenius kinetics, $\frac{1}{\tau} = \nu e^{-E_a/k_B T}$, predicts time scale of microseconds and minutes for event-event time interval (τ) on c^+ and c^-, respectively, at 300 K. Comparing this time with deposition rate brings a physically meaningful picture of deposition. The diffusion coefficient is given by the Einstein relation [13]

$$D = \frac{1}{2d\tau}, \qquad (3)$$

where d is the dimension of the motion of the particle (d=2 in our case). Since a Pd particle hops to an adjacent unit cell by each hopping event, D becomes the number of unit cells the particle visits per unit time. Therefore, Pd adatoms on the c^+ surface will visit about a million surface unit cells per second. 1 ML dosage is equivalent to about 3.5 Pd atoms per unit cell. Even if we assume very fast deposition (for example 0.1 ML/sec), a Pd adatom will travel a very long distance before new atoms are deposited to near positions, so it will be captured by an existing cluster. Conversely, for the c^- surface, Pd atoms almost will not hop until the new adatom is deposited next to it. As a result, very large clusters will be grown on the c^+ surface, but Pd atoms will be dispersed on the c^- surface.

Our kinetic Monte Carlo (KMC) simulations support the aforementioned picture. As Figure 2 c and d show, large clusters are predicted to grow on c^+ while Pd forms a planar structure on c^-. The relative areas that are covered by Pd can be compared with Auger electron spectroscopy (AES), measured by Zhao *et al*. [4]; they observed much stronger Pd signal for the

c^- surface than for the c^+ surface, which indicates Pd on c^- covers much larger area than on c^+. Agreeing with their observations, the relative area, as shown in Figure 2 a and b, is much larger for the c^- surface. Additionally, the curves in the graphs for c^- are very close to the curve of randomly deposited immobile particle in the continuum model. In the latter model, the curve follows a $1\text{-}e^{-x}$ behavior, where x is the dosage in monolayer (ML) unit. This observation agrees with the aforementioned argument based on hopping time for c^-. It should be mentioned that relative areas larger than $1\text{-}e^{-x}$ in Figure 2 a and b are due to finite size effect of Pd atoms; for example, Pd atoms cannot settle on monomers or dimmers, while there is no such size limitation in the continuum model. Note that the relative area of Pd for c^+ might be smaller than that appears in the Figure 2a because the simulation cell size is much smaller than the area that Pd atoms travel before new adatoms are added. The fact that only one cluster, not various sizes of clusters, exists in the cell (Fig. 2c) implies this limitation of our simulations.

The substantial difference in Pd deposition structures between the positive surface and the negative surface is kinetic in origin. The energetics indicates that forming a large cluster is thermally favored to forming a dispersed structure on both surfaces, i.e. zero size of critical nuclei. Palladium atoms on the positive surface move very fast so that they form bulky clusters, as thermodynamics predicts. Conversely, the motions of those on the negative surface are kinetically suppressed, so that they are deposited in a dispersed manner for low dosage, or in a planar manner for high dosage. Cluster sizes depend strongly on the temperature because the event-event interval depends exponentially on the temperature. We observed that large clusters start to form at 400 K for c^-, with many small clusters starting to form for c^+ at 200 K.

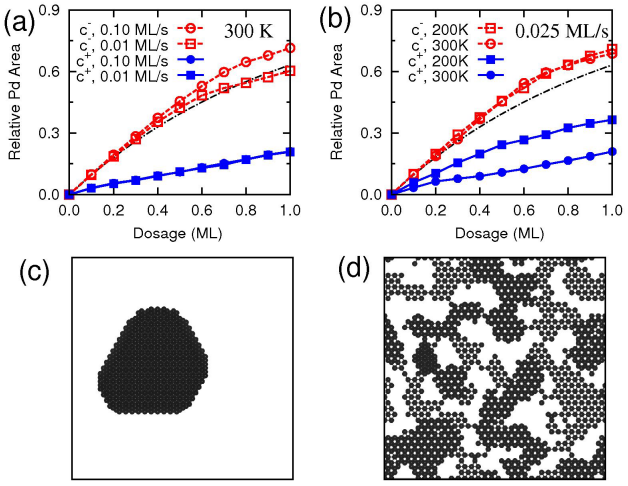

Figure 2 Relative area of the surfaces that are covered by Pd (a) at 300 K and (b) with 0.025 ML/sec deposition rate. Black dash-dot line is the relative area from continuum model of immobile particle, $1\text{-}e^{-x}$. KMC simulated atomic structure of 1 ML dosage for (c) c^+ and (d) c^- surfaces at 300 K when the deposition rate is 0.025 ML/sec. In (d), most parts of Pd are in single layer or double layer, but small triple layer part is there at the center-right of the figure. Reproduced with permission from ref [15].

Even though it is suppressed, Pd atoms on the negative surface move, so one might think that they will form bulky clusters after certain amount of time elapses. However, our KMC simulations of annealing at 300 K demonstrated that cluster sizes are still much smaller than those of c^+ for 0.1 ML, and at 1 ML planar geometry is preserved. At low dosage (0.1 ML in our simulation), most atoms are atomically dispersed right after deposition, but became aggregated in

a few tens of minutes. Yet the clusters are quite small compared to the clusters on the c^+ surface. There are many mobile or immobile clusters near the mobile species after deposition. They form clusters only with close atoms or clusters, in turn, becoming immobile clusters. As a result, clusters on c^- are much smaller than those on c^+, and they cover a much larger area. At high dosage (1 ML in our simulation), after rearrangement of some atoms, all atoms have the bonding configuration that requires two or more Pd-O or Pd-Pd bonds to break to be agglomerated. For instance, the atom at the straight edge of a cluster has four neighbor Pd atoms, and two Pd-Pd bonds and one Pd-O bond need to be broken to move. Exponential dependence on the activation barrier of the transition time allows the planar structure to be stable for a very long period of time.

CONCLUSIONS

We demonstrate that deposition geometries of palladium on the oppositely polarized surfaces of $LiNbO_3$ (0001) are qualitatively different around room temperature. This difference originates from a multiple order of magnitude difference in palladium moving speeds. Low diffusion barriers and negligible agglomeration barriers give rise to forming large clusters on the positive (c^+) surface, while high diffusion and agglomeration barriers cause dispersed or planar geometry on the negative (c^-) surface. Strong palladium bonding to the surface oxygens that are present to passivate the surface charge of the c^- surface leads to the large activation barrier for palladium motion. In contrast to the prevalent explanation that different charging of the metal is the origin of the difference in catalysis of transition metals supported on oppositely polarized substrate, we expect that the geometric difference of the metal induces considerably different catalytic activity.

ACKNOWLEDGMENTS

A. M. Rappe was supported by the Air Force Office of Scientific Research (AFOSR) (FA9550-10-1-0248), S. Kim by US Department of Energy (DOE) (DEFG02-07ER15920), and M. R. Schoenberg by National Science Foundation (NSF) MRSEC Program (DMR11-20901). Computational support was provided by High Performance Computing Modernization Program Office (HPCMO) of US Department of Defense.

REFERENCES

1. Y. Inoue, I. Yoshioka, and K. Sato, *J. Phys. Chem.* **88**, 1148 (1984)
2. C. Noguera, *J. Phys.:Condens. Matter* **12**, R367 (2000)
3. J. K. Nørskov, T. Bligaard, B. Hvolbæk, F. Abild-Pedersen, I. Chorkendorff, and C. H. Christensen, *Chem. Soc. Rev.* **37**, 2163 (2008)
4. M. H. Zhao, D. A. Bonnell, and J. M. Vohs, *J. Vac. Sci. Technol. A* **27**, 1337 (2009)
5. Y. Yun, N. Pilet, U. D. Schwarz, and E. I. Altman, *Surf. Sci.* **603**, 3145 (2009)
6. A. Saito, H. Matsumoto, S. Ohnisi, M. Akai-Kasaya, Y. Kuwahara, and M. Aono, *Jap. J. Appl. Phys.* **43**, 2057 (2004)
7. S. V. Levchenko and A. M. Rappe, *Phys. Rev. Lett.* **100**, 256101 (2008)
8. J. P. Perdew, K. Burke, and M. Ernzerhof, *Phys. Rev. Lett.* **77**, 3865 (1996)
9. A. M. Rappe, K. M. Rabe, E. Kaxiras, and J. D. Joannopoulos, *Phys. Rev. B 41*, 1227 (1990)
10. N. J.Ramer and A.M.Rappe,*Phys. Rev. B* 59, 12471 (1999)

11. G. Henkelman, B. P. Uberuaga, and H. Jónsson, *J. Chem. Phys.* **113**, 9901 (2000)
12. P. Giannozzi *et al.*, *J. Phys. Condens. Matter* **21**, 395502 (2009)
13. H. Brune, *Surf. Sci. Rep.* **31**, 121 (1998)
14. B. Hammer, Y. Morikawa, and J. K. Nørskov, *Phys. Rev. Lett.* **76**, 2141 (1996)
15. S. Kim, M. R. Schoenberg, and A. M. Rappe, *Phys. Rev. Lett.* **107**, 076102 (2011)